

Comparison of Normal and Inverted Band Structure HgTe/CdTe Superlattices for Very Long Wavelength Infrared Detectors

C.H. GREIN,^{1,3} H. JUNG,¹ R. SINGH,¹ and M.E. FLATTÉ²

1.—EPIR Technologies, Bolingbrook, IL 60440. 2.—Department of Physics and Astronomy, University of Iowa, Iowa City, IA 52242. 3.—E-mail: grein@epir.com

The type III band alignment of HgTe/CdTe superlattices leads to the interesting possibility of achieving very long wavelength infrared (VLWIR) (15 μm and longer) cutoff wavelengths with either normal (HgTe layer thickness less than about 70 Å for CdTe layer thickness of 50 Å) or inverted (HgTe thickness greater than about 70 Å) band structures. The inverted band structure superlattices promise even greater cutoff wavelength control than the normal band structure ones. However, the electronic band gaps of inverted band structure superlattices are substantially less than their optical band gaps, leading to large thermal carrier concentrations even at temperature as low as 40 K. These high carrier concentrations in turn give rise to more rapid Auger recombination than normal band structure superlattices with the same cutoff wavelengths. We conclude that the highest performance is expected from VLWIR HgTe/CdTe superlattice-based detectors with normal band structure absorber layers.

Key words: HgTe/CdTe, superlattices, very long wavelength infrared (VLWIR), detectors

INTRODUCTION

HgTe/CdTe superlattices have long been of interest as absorbers in infrared photon detectors. Early predictions^{1,2} of desirable features such as low tunneling currents, sharp optical absorption onsets, and good control over the cutoff wavelength led to extensive growth efforts^{3–7} and the successful demonstrations of HgTe/CdTe-based infrared detectors and lasers. However, little effort has been devoted to examining the potential of HgTe/CdTe superlattices for very long wavelength infrared (VLWIR: 15 μm and longer) detection. It is perhaps at VLWIR wavelengths that the superlattices have their greatest potential for the above reasons.⁸ This work focuses on the modeling of VLWIR HgTe/CdTe superlattices grown on CdTe substrates. In addition, experimental results on two such superlattices are summarized. For relatively thin HgTe layer thicknesses, the superlattice electronic band structures are normal,

namely, the lowest energy band with condition symmetry (C1) lies higher in energy than the highest with hole-like symmetry (HH1). However, the type III band alignment of the superlattices (HgTe is a semimetal and CdTe is a semiconductor) results in thick HgTe-layer thickness superlattices having an inverted band structure reflecting that of bulk HgTe, namely, C1 is lower in energy than HH1.

Incidentally, it has been shown that some Hg is incorporated in the CdTe layers during MBE growth since the Hg cell shutter is left open during the CdTe growth in order to prevent Hg evaporation from the layer. The Hg composition in the CdTe layers has been found to be 5–15% depending on growth conditions and crystallographic orientation.^{9,10} Therefore, in HgTe/CdTe superlattices, it is expected that Hg will be unintentionally incorporated in the CdTe layers.

THEORETICAL METHODS

The electronic band structures were computed employing an envelope-function-based 14-band K-p method with a 40 K valence band offset of 554 meV⁸

(Received October 7, 2004; accepted December 1, 2004)

and a (211) crystal orientation. The barrier layers are assumed to be $\text{Hg}_{0.05}\text{Cd}_{0.95}\text{Te}$ based on the above discussion. The highly nonparabolic band structures and momentum matrix elements are used directly as input for the computation of Auger lifetimes. They are input into the Auger rate computations in the form of look-up tables with a mesh spacing of 0.002 \AA^{-1} . The principal methods employed are discussed in Ref. 11, and have been extended to include the effects of superlattice Umklapp processes.¹² Umklapp processes are negligible in bulk direct gap systems.¹³ However, due to the large size of the superlattice unit cells and hence the small size of reciprocal lattice vectors in the growth-axis direction, Umklapp processes have been shown to contribute approximately half of the total rate of Auger recombination in superlattices.¹² The transition matrix elements are evaluated using a statically screened Coulomb interaction and first-order $k \cdot p$ for the wave function overlaps. The multidimensional k -space integrals are evaluated employing an adaptive mesh Monte Carlo algorithm.

Radiative lifetimes were also computed employing directly the band structures and matrix elements from the 14 band $k \cdot p$ formalism, and evaluated with the standard van Roosbroeck–Shockley expression¹⁴ that does not take photon recycling into account.

Defect-mediated recombination is not included in the calculations; hence, the reported lifetimes are theoretical upper bounds designed to provide guidance to experimental programs in assessing their materials quality. Also, they help in eliminating unattractive systems.

THEORETICAL RESULTS

The type III band alignment of HgTe/CdTe superlattices leads to the possibility of achieving VLWIR cutoff wavelengths with either normal (HgTe layer thickness less than about 70 \AA for CdTe layer thickness of 50 \AA) or inverted (HgTe thickness greater than about 70 \AA) band structures (Fig. 1). A more detailed description of normal and inverted band structure superlattices is found in Ref. 8. The portion of the curve in Fig. 1 corresponding to normal band structures ($d_w < 70 \text{ \AA}$) has a much greater slope than the inverted portion in the wavelength range of interest (i.e., $15\text{--}40 \mu\text{m}$). This implies that a small change ($<5 \text{ \AA}$) in HgTe thickness will cause a larger change in the cutoff wavelength of a normal band structure superlattice than of an inverted band structure superlattice. Hence, it is easier to control the VLWIR cutoff wavelength of an inverted band structure superlattice. Specifically, a $17 \mu\text{m} \pm 1 \mu\text{m}$ optical cutoff with a normal band structure superlattice requires that the well thickness be controlled to 1.7% of its value, whereas an inverted band structure superlattice requires 7.7% precision. For comparison, a HgCdTe alloy would need 0.1% compositional control. Hence, inverted band structure superlattices promise better control over VLWIR cutoff wavelengths. Note that the atomic discreteness prohibits continuous variations of

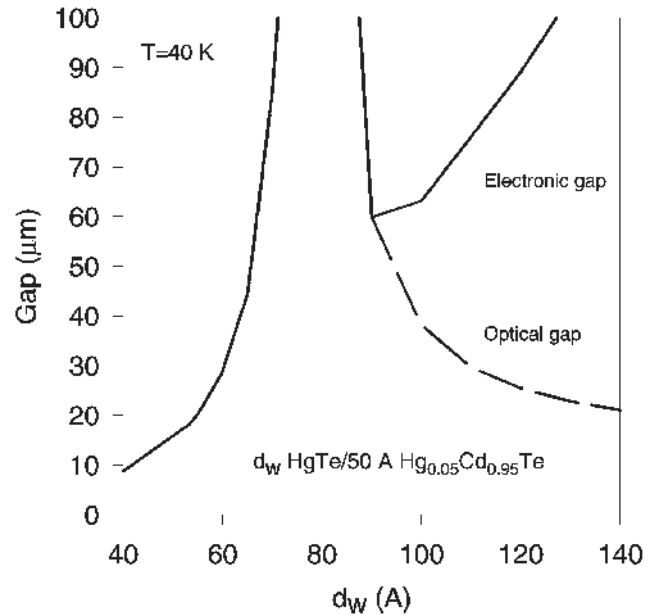


Fig. 1. Computed zone center electronic band gaps (solid line) and optical band gaps (dashed line) (plotted in terms of wavelength) of $\text{HgTe}/\text{Hg}_{0.05}\text{Cd}_{0.95}\text{Te}$ superlattices with HgTe layer thicknesses of d_w and $\text{Hg}_{0.05}\text{Cd}_{0.95}\text{Te}$ layer thicknesses of 50 \AA . The electronic and optical gaps are the same for d_w less than approximately 90 \AA .

layer thicknesses; hence, achievable cutoff variations may be greater than these theoretical predictions.

However, selection rules result in the optical band gaps of inverted band structure superlattices being substantially greater than their electronic band gaps, and the small electronic gaps lead to large thermal carrier concentrations even at temperatures as low as 40 K . These high carrier concentrations in turn give rise to more rapid Auger recombination than normal band structure superlattices with the same cutoff wavelengths.

Calculations of the recombination lifetimes of a normal band structure ideal (defect-free) 60 \AA $\text{HgTe}/50 \text{ \AA}$ $\text{Hg}_{0.05}\text{Cd}_{0.95}\text{Te}$ superlattice were made. It has a fundamental band gap (HH1-C1) equal to its optical absorption cutoff, both $28.8 \mu\text{m}$ at 40 K . We find with an acceptor concentration of $5 \times 10^{15} \text{ cm}^{-3}$ that the hole-hole Auger lifetime is $7.0 \times 10^{-9} \text{ s}$, and the electron-electron Auger lifetime is over 1 sec. The electronic band structure for this superlattice showing the positions of the carriers most likely to take part in hole-hole Auger transitions is plotted in Fig. 2. The transitions are spread over a substantial portion of the Brillouin zone, implying some Auger suppression is present.

For comparison, calculations of the carrier recombination lifetimes in an ideal 110 \AA $\text{HgTe}/50 \text{ \AA}$ $\text{Hg}_{0.05}\text{Cd}_{0.95}\text{Te}$ superlattice at 40 K with an acceptor concentration of $5 \times 10^{15} \text{ cm}^{-3}$ give a hole-hole Auger lifetime of $1.6 \times 10^{-10} \text{ s}$ and an electron-electron Auger lifetime of $9.0 \times 10^{-10} \text{ s}$. The superlattice has an optical cutoff wavelength (HH1-C1) of $29.7 \mu\text{m}$ at 40 K , very close to that of the normal band structure superlattice of Fig. 2. Figure 3 shows that hole-hole Auger recombination is very fast: the involved

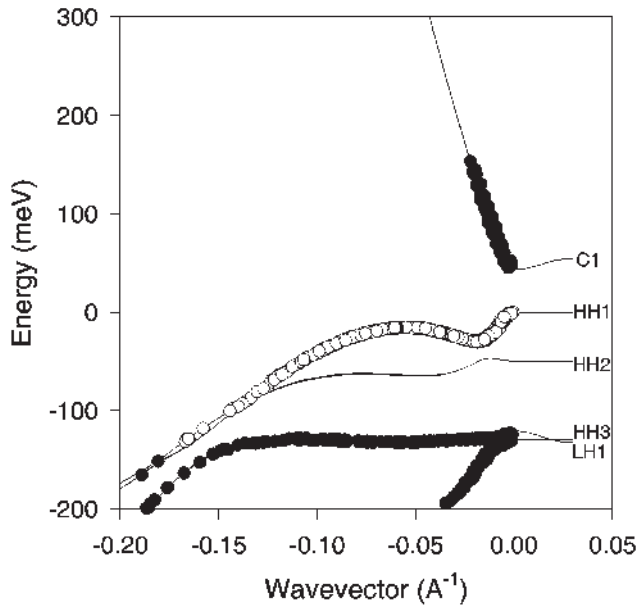


Fig. 2. Computed electronic band structure of a 60 Å HgTe/50 Å Hg_{0.05}Cd_{0.95}Te superlattice with 28.8- μ m optical cutoff wavelength at 40 K. The growth-axis bands are plotted with positive wavevectors, and the in-plane bands are plotted with negative wavevectors. Holes (hollow circles) and electrons (solid circles) most likely to take part in hole-hole (acceptor concentration 5×10^{15} cm⁻³) Auger recombination transitions are superimposed on the bands.

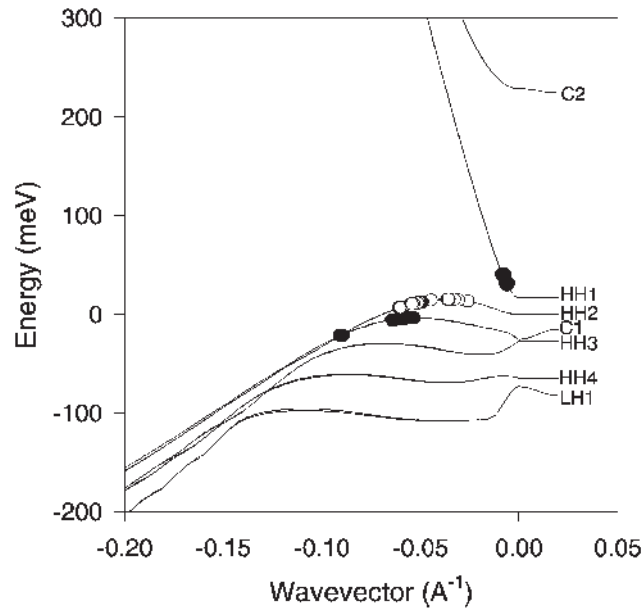


Fig. 3. Computed electronic band structure of a 110 Å HgTe/50 Å Hg_{0.05}Cd_{0.95}Te superlattice with 29.7- μ m optical cutoff wavelength at 40 K. Holes (hollow circles) and electrons (solid circles) most likely to take part in hole-hole (acceptor concentration 5×10^{15} cm⁻³) Auger recombination transitions are superimposed on the bands.

carriers are tightly confined to small regions of the Brillouin zone where their occupation probabilities are high. Moreover, the small electronic energy gap (HH2-HH1, 16.3 meV or 76.1 μ m) implies high thermal carrier concentrations (approximately 7×10^{16} cm⁻³), even at 40 K. Hence, it is no surprise that the Auger lifetimes are very short.

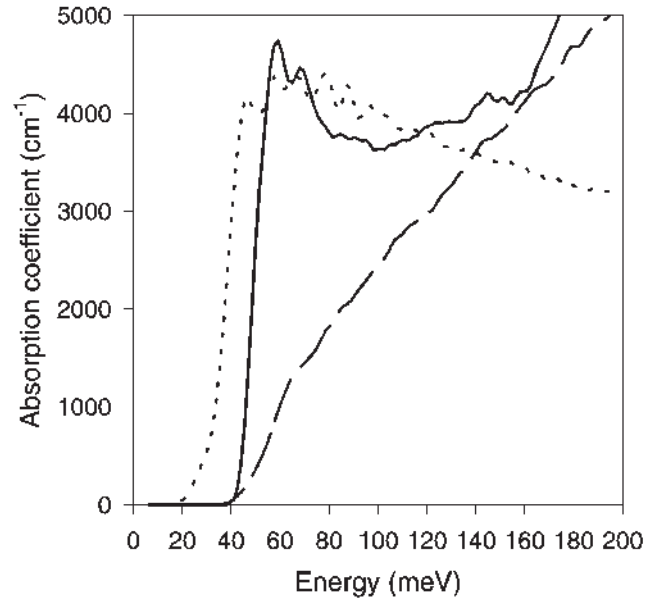


Fig. 4. Computed fundamental optical absorption spectra of two superlattices (solid line for a normal band structure 60 Å HgTe/50 Å Hg_{0.05}Cd_{0.95}Te superlattice; dotted line for an inverted band structure 110 Å HgTe/50 Å Hg_{0.05}Cd_{0.95}Te superlattice) and bulk HgCdTe alloy (dashed line), all with optical band gaps of approximately 40 meV at 40 K.

Figure 4 plots the computed optical absorption spectra of the normal band structure 60 Å HgTe/50 Å Hg_{0.05}Cd_{0.95}Te and inverted band structure 110 Å HgTe/50 Å Hg_{0.05}Cd_{0.95}Te superlattices at 40 K. Included as well is the absorption of a HgCdTe alloy with the same cutoff as the normal band structure superlattice. The figure verifies that the two superlattices have essentially the same optical cutoff wavelengths despite their different electronic band gaps. The comparison with HgCdTe alloy verifies the stronger optical absorption onsets of the superlattices.

Figure 5 plots the computed total recombination lifetimes for the same range of superlattices as in Fig. 1 and for an acceptor concentration of 5×10^{15} cm⁻³. It clearly shows a general trend of longer lifetimes of the normal band structure ones.

EXPERIMENTAL RESULTS

Two HgTe/CdTe superlattice structures, MCT00156 and MCT00236, were grown to 200 periods on (211) CdTe/Si substrate using a 32P Riber MBE system (Rueil-Malmaison, France) and characterized, as described in a previous work.¹ Both were n-type doped with In, and the as-grown superlattices were characterized. The measured absorption coefficient for sample MCT00156 is shown in Ref. 1. It gives a cutoff energy $E_{\text{cutoff}} = 140.1$ meV (8.49 μ m) at 300 K, which shifts to $E_{\text{cutoff}} = 55$ meV (22.54 μ m) at 40 K. The X-ray diffraction double-crystal rocking curve (DCRC) full width at half maximum (FWHM) of MCT00156 was measured to be 42 arcsec. The DCRC shows two main peaks and two satellite peaks. The main peaks are associated with the substrate and the superlattice, while the two satellite peaks (one on each side of

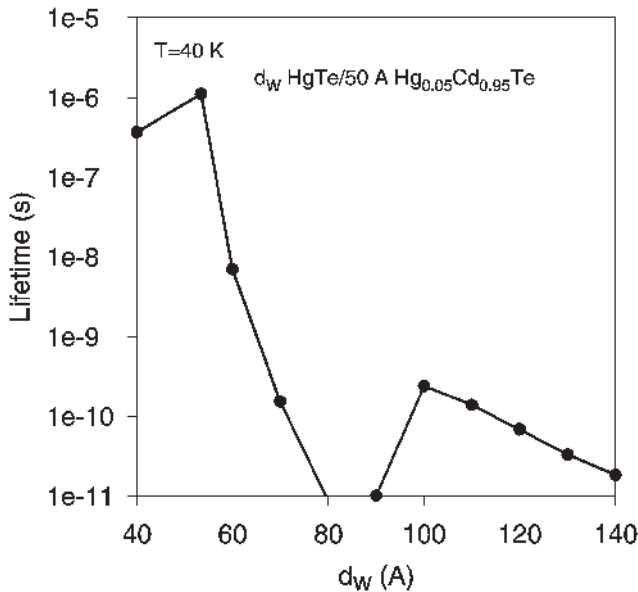


Fig. 5. Computed recombination lifetimes at 40 K of HgTe/ $\text{Hg}_{0.05}\text{Cd}_{0.95}\text{Te}$ superlattices with HgTe layer thicknesses of d_w and $\text{Hg}_{0.05}\text{Cd}_{0.95}\text{Te}$ layer thicknesses of 50 Å with an acceptor concentration of $5 \times 10^{15} \text{ cm}^{-3}$.

the central Bragg peak) provide information on the average thickness of the well and barrier layers. The positions of the satellite peaks of sample MCT00156 yield HgTe well and CdTe barrier average thickness of 52 Å and 51 Å, respectively. An average HgTe well thickness of less than 70 Å indicates a normal band structure superlattice has been grown. MCT00236 is an inverted gap superlattice with targeted layer thicknesses of 100 Å HgTe and 50 Å CdTe, producing an optical band gap similar to that of MCT00156. The photoconductive decay method was used for minority carrier lifetime measurements. Temperature-dependent experimental lifetime data are presented in Fig. 6 for the normal band structure superlattice. A comparison with the theoretical lifetime leads to the conclusion that Shockley–Read–Hall recombination is the dominant recombination pathway in this sample. The signal from the lifetime measurements on the inverted band structure superlattice (MCT00236) was below the detection level of the system, which is capable of reliably measuring lifetimes as short as 10 ns.

SUMMARY

The electronic band structures, optical absorption spectra, and intrinsic recombination lifetimes of inverted and normal band structure HgTe/CdTe superlattices were theoretically modeled. Both types of HgTe/CdTe superlattices were also grown and characterized. Even though inverted band structure superlattices promise better control over cut-off wavelengths, their Auger recombination lifetimes are

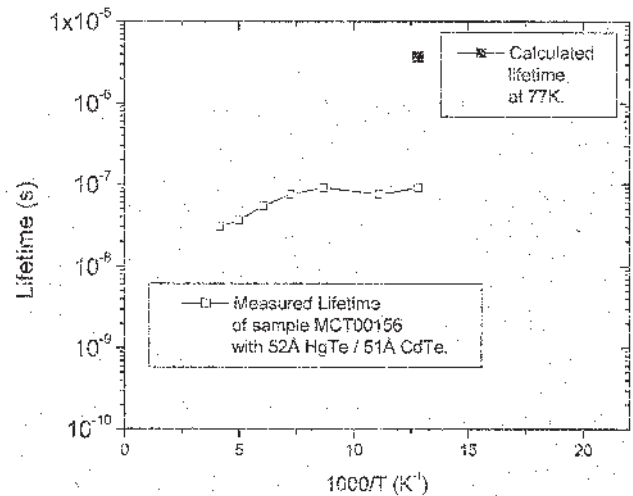


Fig. 6. Measured recombination lifetimes of the normal band structure superlattice MCT00156, together with calculated lifetime at 77 K.

much shorter than those for normal band structure superlattices. We conclude that normal band structure HgTe/CdTe superlattices are more promising for VLWIR detector applications.

ACKNOWLEDGEMENTS

We thank the Air Force Research Laboratory for supporting this work under AFRL/MLPS Contract No. FA8650-04-C-5423.

REFERENCES

1. J. Schulman and T.C. McGill, *Appl. Phys. Lett.* 34, 663 (1979).
2. D.L. Smith, T.C. McGill, and J.N. Schulman, *Appl. Phys. Lett.* 43, 180 (1983).
3. J.P. Faurie, A. Million, and J. Piagnet, *Appl. Phys. Lett.* 41, 713 (1982).
4. J. Reno and J.P. Faurie, *Appl. Phys. Lett.* 49, 409 (1986).
5. X. Chu, S. Sivananthan, and J.P. Faurie, *Superlattices Microstruct.* 4, 173 (1988).
6. K.A. Harris, T.H. Myers, R.W. Yanka, L.M. Mohnkern, and N. Otsuka, *J. Vac. Sci. Technol. B* 9, 1982 (1991).
7. C.A. Hoffman, J.R. Meyer, R.J. Bartoli, X. Chu, J.P. Faurie, L.R. Ram-Mohan, and H. Xie, *J. Vac. Sci. Technol. A* 8, 1200 (1990).
8. C.R. Becker, V. Latussek, G. Landwehr, and L.W. Molenkamp, *Phys. Rev. B* 68, 035202 (2003).
9. J. Reno, R. Sporken, Y.J. Kim, C. Hsu, and J.P. Faurie, *Appl. Phys. Lett.* 51, 1545 (1987).
10. R.H. Hartley, M.A. Folkard, D. Carr, P.J. Orders, D. Rees, I.K. Varga, V. Kumar, G. Shen, T.A. Steele, H. Buskes, and J.B. Lee, *J. Cryst. Growth* 117, 166 (1992).
11. C.H. Grein, P.M. Young, M.E. Flatté, and H. Ehrenreich, *J. Appl. Phys.* 78, 7143 (1995).
12. M.E. Flatté, C.H. Grein, T.C. Hasenberg, S.A. Anson, D.-J. Jang, J.T. Olesberg, and T. Boggess, *Phys. Rev. B* 59, 5745 (1999).
13. S. Brand and R.A. Abram, *J. Phys. C* 17, L571 (1984).
14. W. van Roosbroeck and W. Shockley, *Phys. Rev.* 94, 1558 (1954).
15. H.S. Jung, C.H. Grein, and C.R. Becker, *Proc. SPIE* 5209, 90 (2003).